Extreme Mechanics Letters 73 (2024) 102269

Contents lists available at ScienceDirect

Extreme Mechanics Letters

journal homepage: www.elsevier.com/locate/eml

Automated de novo design of architectured materials: Leveraging eXplainable Artificial Intelligence (XAI) for inspiration from stochastic microstructure outliers

Zhengkun Feng [a], Weijun Lei [b], Leidong Xu [a], Shikui Chen [b], Hongyi Xu [a,*]

[a] School of Mechanical, Aerospace, and Manufacturing Engineering, University of Connecticut, Storrs, CT 06269, United States
[b] Department of Mechanical Engineering, State University of New York at Stony Brook, Stony Brook, NY 11794, United States

ARTICLE INFO

Keywords:
Architectured materials
XAI
Stochastic microstructures
Periodic microstructures
Generative design
Design inspiration

ABSTRACT

Engineered architectured Materials, such as metamaterials with periodic patterns, achieve superior properties compared with their stochastic counterparts, such as the random microstructures found in natural materials. The primary research question focuses on the feasibility of learning advantageous microstructural features from stochastic microstructure samples to facilitate the generative design of periodic microstructures, resulting in unprecedented properties. Instead of relying on brainstorming-based, *ad hoc* design inspiration approaches, we propose an eXplainable Artificial Intelligence (XAI)-based framework to automatically learn critical features from the exceptional outliers (with respect to properties) in stochastic microstructure samples, enabling the generation of novel periodic microstructure patterns with superior properties. This framework is demonstrated on three benchmark cases: designing 2D cellular metamaterials to maximize stiffness in all directions, to maximize the Poisson's ratio in all directions, and to minimize the thermal expansion ratio. The effectiveness of the design framework is validated by comparing its novel microstructure designs with known stochastic and periodic microstructure designs in terms of the properties of interest.

1. Introduction

In architectured material design, a compelling research question arises: How can knowledge and data acquired from one category of microstructures inform the design of microstructures in a different category to achieve superior properties? This study focuses on leveraging knowledge learned from stochastic microstructures to facilitate property-driven generative design of periodic microstructures (e.g. cellular metamaterials). Stochastic microstructures are random in nature and typically fabricated using methods that do not lend themselves to the direct control of microstructure. Examples of stochastic microstructures include nanoparticle composites [1–3], chopped fiber composites [4,5], porous polymers and foams [6–10], coral-like random structures via directional ice templating [11], and many more. Periodic microstructures consist of repeating cellular units that are highly engineered for tailorable properties. Examples of periodic microstructures include the engineered metamaterials [12,13] and lattice structures [14,15].

In literature, brainstorming-based, *ad hoc* approaches have been extensively employed to draw inspirations from natural/biological materials for designing metamaterials and architectured materials [16–21]. These approaches often involve proposing novel periodic microstructures by mimicking structural features observed in stochastic natural materials, relying on inspiration and reasoning, which constitutes a manual process.

On the other hand, the literature includes a significant number of works on computational design approaches that enable microstructure design automation. For the freeform design of periodic microstructures, topology optimization based on pixelated/voxelated density fields [22–24] or level set functions [25,26] has been widely applied for generating novel microstructure patterns with maximum stiffness, negative Poisson ratio, negative thermal expansion ratio, etc. For the design of stochastic microstructures, statistical characterization and stochastic reconstruction methods have been proposed for defining the design space with statistical microstructure descriptors. Popular statistical microstructure descriptors include *ad hoc* microstructure parameters [4,5,27–29], *N*-point correlation functions [30–33], spectrum density function [34,35], and random fields [36,37]. In recent years,

* Corresponding author.
E-mail address: hongyi.3.xu@uconn.edu (H. Xu).

https://doi.org/10.1016/j.eml.2024.102269
Received 31 July 2024; Received in revised form 12 October 2024; Accepted 22 November 2024
Available online 26 November 2024

deep generative models, Generative Adversarial Network (GAN) and Variational Autoencoder (VAE), also see increasing applications in designing both periodic [38–43] and stochastic [44–50] microstructures. In our recent works, we investigated deep generative model [51] and curvature functionals [52,53] approaches in establishing a unified design space that embodies multiple categories of microstructures, including both periodic and stochastic microstructures, for freeform design.

However, the aforementioned works do not provide a rational approach for leveraging the knowledge learned from stochastic microstructures to guide the design of periodic structures. To resolve this issue, we propose and validate an eXplainable Artificial Intelligence (XAI)-based framework for generative design of novel periodic microstructure based on stochastic microstructure exemplars. Instead of treating the input-output relationship as a black box, XAI [54,55] provides an explainability of the causal relationship between microstructure features as the input and the material properties as the output. Our hypothesis posits that by learning advantageous microstructure features from stochastic microstructure data using XAI, novel periodic microstructure designs created by arranging those advantageous features in a periodic manner can achieve superior properties compared to stochastic microstructures. The motivation is to learn critical features from one microstructure category (e.g., stochastic microstructures) to inspire new designs in another category (e.g., deterministic metamaterial units) where data is lacking. In this work, a novel XAI-based framework is proposed to automate the process of designing periodic microstructures inspired by advantageous features learned from stochastic microstructure data. This framework is implemented in three benchmark cases to test our hypothesis.

2. methodologies of xai construction and design generation

2.1. Overview of the proposed XAI-based microstructure design framework

The proposed framework (Fig. 1) embodies three major components: (a) stochastic microstructure database, (b) supervised learning of microstructure-property relationship and Gradient-weighted Regression Activation Mapping (Grad-RAM) [56,57] for critical microstructure feature identification, and (c) a skeletonization-based periodic microstructure construction approach.

We established a stochastic microstructure database that includes 20,000 2D stochastic microstructure images [51] in four categories: random particle, random fiber, random porous, and random spinodal structures. The microstructure samples are generated by stochastic reconstruction methods [1,4,58–60], details of which will be introduced in the method section. Additionally, the database includes the properties of all microstructure samples obtained by Finite Element Analysis.

Convolutional Neural Networks (CNN) are trained as the regressors that predict the material properties based on input microstructure images. Transfer learning on a modified ResNet-18 model [61] is conducted to create the regressors (Figures S1 and S2). In addition to the prediction accuracy, interpretability is also crucial for building trust in these networks. It is important to build 'transparent' models that can explain the key factors driving the predictions. With the trained CNN regressors, an XAI method, Grad-RAM, is employed to identify the

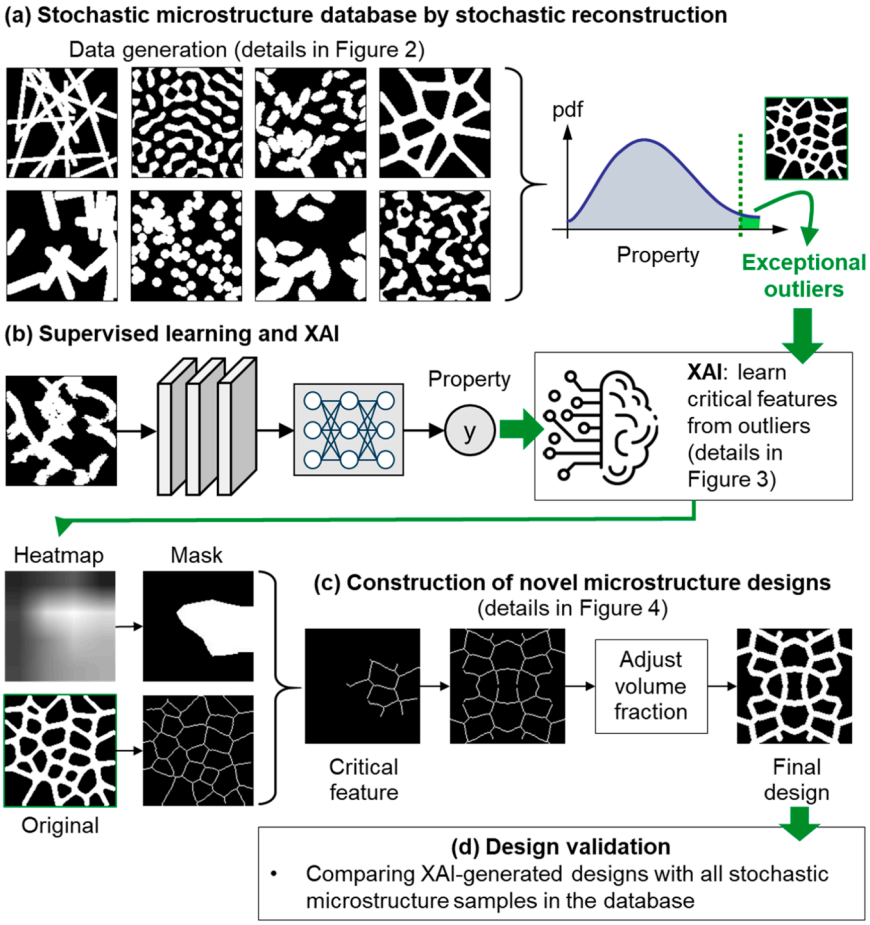

Fig. 1. Overview of the proposed XAI-based design automation framework for architectured materials. (a) A highly diverse stochastic microstructure database created by stochastic reconstruction algorithms. (b) Supervised learning for property prediction and XAI for identifying critical microstructure features leading to desired properties. (c) Construction of novel microstructure designs with critical microstructure features.

critical local regions in the microstructure images that explain the model output, to be specific, the local regions that contribute to the regression results. Grad-RAM is a method that was developed based on Gradient-weighted Class Activation Mapping (Grad-CAM). Grad-CAM visualizes class activation maps in classification tasks. For a specific convolutional layer l, Grad-CAM calculates the gradient of the target class (y^c) score with respect to the feature map A_k^l of it.

$$gradient = \frac{\partial y^c}{\partial A_k^l} \tag{1}$$

The gradients indicate which neurons in the layer have the most influence on the final prediction. Grad-CAM computes α_k^c, a weighted average of the gradients for each feature map channel, creating a weight for each channel based on its importance to the target class using the following equation:

$$\alpha_k^c = \frac{1}{Z}\sum_i\sum_j \frac{\partial y^c}{\partial A_{k.ij}^l} \tag{2}$$

where Z is the total number of pixels. These weights are combined with the feature maps to create a weighted activation map, $L^c_{\text{Grad}-\text{CAM}}$, which is upsampled to the original image size to highlight the area's most relevant for the class.

$$L^c_{Grad-CAM} = ReLU(\sum\nolimits_k \alpha_k^c A_k^l) \tag{3}$$

The result will be a heatmap showing which parts of the image the network focused on for that prediction. Therefore, Grad-CAM can provide insights into the abstract features or patterns that specific neurons or layers respond to, and reveal the visual features that the network has learned.

In contrast to Grad-CAM that has been explained above and computes gradients with respect to specific classes in classification tasks, Grad-RAM calculates gradients based on the predicted continuous output in regression tasks. Let f be CNN model (regressor) that predict the material properties of interest y based on the input image x, and g denotes a regression result of interest, the purpose of Grad-RAM is to explain the output of the model for a given input $f(x)$ through a visual explanation map generated by:

$$L^g_{\text{Grad}-\text{RAM}} = \text{ReLU}\left(\sum_k \alpha_k \bullet A^k\right) \tag{4}$$

$$\alpha_k = \frac{1}{Z}\sum_i\sum_j \frac{\partial y}{\partial A_{ij}^k} \tag{5}$$

Where A_k represents the k-th feature map of the selected convolutional layer, y is the output the CNN model, α_k is the pooling gradients for neuron importance weights, Z is the number of elements in each feature map. Applying ReLU ensures that only features having a positive influence on the output are considered. In terms of computational complexity, the primary cost of the proposed framework comes from training the CNN regressor. The implementation of Grad-RAM only requires gradient calculations, which incur negligible computational cost.

With microstructure samples with superior properties (exceptional outliers), we employ Grad-RAM to generate heatmaps that pinpoint critical local regions, which embody advantageous microstructure features contributing to desirable properties. These critical local regions serve as fundamental microstructure units for constructing novel periodic microstructure designs, which is the last step of the framework. The novel designs obtained will undergo validation through comparison with established designs to assess their properties.

2.2. Creation of stochastic microstructure database by stochastic reconstruction

We have created a database of 20,000 2D stochastic microstructure images [51] by stochastic reconstruction. The images have a resolution of 128 × 128 pixels, with the volume fraction (percentage of the white pixels in the entire image) ranging between 0.38 and 0.41. The stochastic microstructure images in our training database generally fall into four categories: random particle-like patterns, random fiber-like patterns, random cellular-like patterns, and random amorphous patterns. Three sets of microstructure reconstruction methods [1,4,58–60] have been employed (Fig. 2).

Firstly, the parametric descriptor-based method [1,3,4,58,62] is applied to create microstructures consisting of random particle types, including spherical and ellipsoidal particles, as well as random fiber-type microstructures. This method focuses on using predefined geometric descriptors to model the spatial arrangement and shape of the microstructural features.

Secondly, the space tessellation-based method [58,63,64] is applied to generate microstructures that resemble random networks and random porous structures. This approach partitions space into multiple zones or cells, each representing a unique phase or component of the material, thus effectively modeling complex interconnected or porous architectures.

Thirdly, the spectrum density function (SDF)-based method [34,35,65] is employed to generate stochastic spinodal-like microstructures. The SDF method characterizes the spatial correlations between pixels of each material phase in the frequency domain. Defining a binary image as $Z(\boldsymbol{r})$, where $\boldsymbol{r}$ represents pixel locations and pixels take values of 0 or 1 (which represent the two material phases), the image's Fourier spectrum is:

$$\mathscr{F}\{Z(\boldsymbol{r})\} = \int_{\mathbb{R}^n} Z(\boldsymbol{r}) e^{-2\pi i \boldsymbol{r}\bullet\mathbf{k}} \mathbf{d}\boldsymbol{k} = \boldsymbol{A_k} \bullet \boldsymbol{e}^{i\phi_k} \tag{6}$$

where $A_{\boldsymbol{k}}$ and $\phi_{\boldsymbol{k}}$ represent the magnitude and phase information at each location $\boldsymbol{k}$ of the Fourier spectrum. For a microstructure image, its SDF $\rho(k)$ is expressed as:

$$\rho(\boldsymbol{k}) = |\mathscr{F}\{Z(\boldsymbol{r})\}|^2 = \boldsymbol{A_k}^2 \tag{7}$$

The mathematical relationship between SDF and the 2-point correlation function, which is a well-established approach for characterizing stochastic images [66–69], has been established by Chatfield [70]. To reconstruct random but statistically equivalent microstructures based on a target SDF, a Gaussian random field approach is employed. The reconstructed microstructure image $Z(\boldsymbol{r})$ is represented by a Gaussian random field $Y(\boldsymbol{r})$, and a numerical realization of $Y(\boldsymbol{r})$ can be obtained using the wave-form method [71]:

$$Y(\boldsymbol{r}) = \sqrt{\frac{2}{N}} \bullet \sum_{i=1}^{N} \cos(k_i \boldsymbol{k}_i \bullet \boldsymbol{r} + \phi_i) \tag{8}$$

where N is the number of terms in the truncated series, ϕ_i is generated by sampling uniform distribution in the range of $[0, 2\pi]$, $\boldsymbol{k}_i$ is a vector uniformly distributed on a unit sphere, and k_i is a scalar obtained by sampling the probability density function $\rho(\boldsymbol{k}) \bullet \boldsymbol{k}$ in the range of $(0, \infty)$.

2.3. Supervised learning models of the microstructure-property relationship

A fundamental component of the Grad-RAM-based design framework is a supervised learning model that predicts the microstructure-property relationship. Convolutional Neural Networks (CNNs) serve as a prominent choice for supervised learning, capable of being trained with the generated data outlined in the previous section. In this study, a regression model based on Residual Network-18 (ResNet-18) is trained

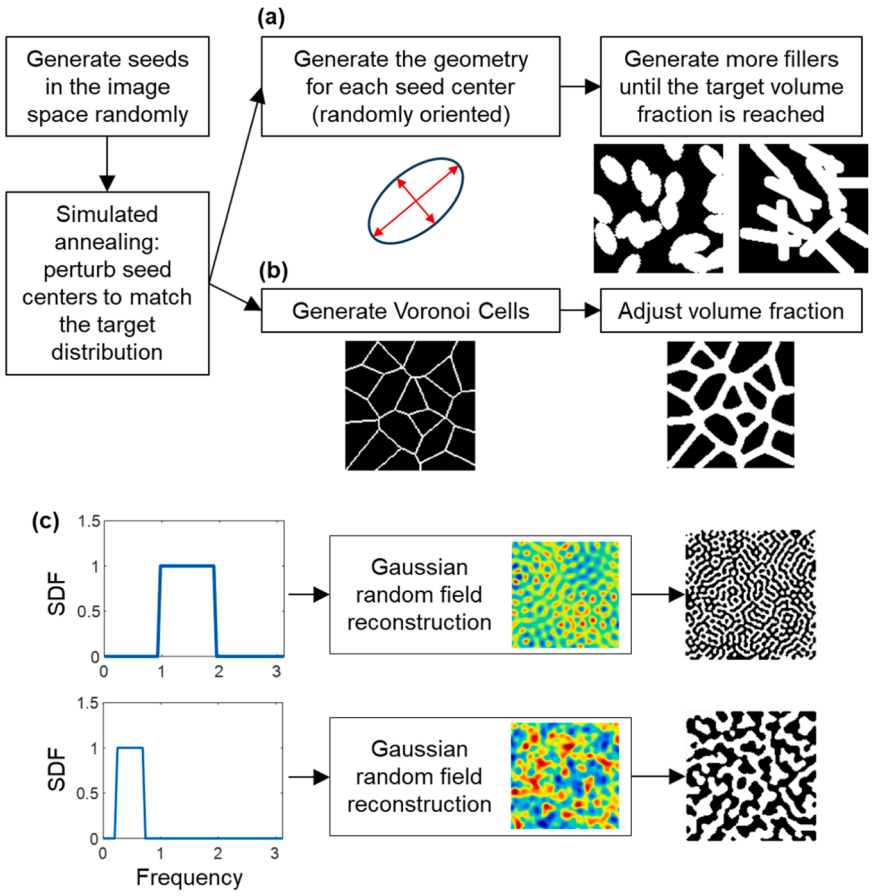

Fig. 2. Different methods which used to generate the stochastic samples: (a) Statistical microstructure parameter-based reconstruction, and (b) Stochastic Voronoi tessellation-based reconstruction, and (c) Generation of various microstructure samples by varying the input spectrum density function.

to predict microstructure properties based on microstructure images (Figure S3). The basic ResNet-18 consists of 18 layers with weights and 8 residual blocks. Within each block, the input traverses through convolutional layers before being added back prior to the final activation function. This unique "residual" connection facilitates the training of deeper networks. Grad-RAM will be applied to identify the critical features from the last convolutional layer. The CNN model is implemented in PyTorch. For all the 20000 samples, 80 % of them are used as training set and the rest 20 % are considered as test set. As listed in Table 2, all supervised learning models have a reasonable level of accuracy in predicting properties of interest. The Mean Squared Error (MSE) loss function which is used in the training is given as:

$$loss = \frac{1}{n}\sum_{i=1}^{n}(y_i - \hat{y}_i)^2 \tag{9}$$

Where y_i is the true value and the $\hat{y}_i$ is the predicted value from the model. As listed in Table 2, all supervised learning models have a reasonable level of accuracy in predicting properties of interest. More details of model training and the structure of this CNN model are listed in Table 1 and Figure S4.

In order to prepare the data for training, we carried out the finite element (FE) simulations. Based on the image structures we generated, the meshes of models are converted from binary microstructure images, where each pixel corresponds to one quadrilateral element. Thus, an image of 128 × 128 pixels is converted a FE mesh with 16384 elements. The material properties used in the simulations are listed in the following Table 3. MAT 1 represents the properties of the white phase and MAT 2 represents the properties of the black phase.

Table 2
Accuracies of the supervised learning models for property prediction. Model 1 and 2 predict Young's modulus along X and Y directions, respectively. Model 3 and 4 predict the Poisson's ratio along X and Y directions, respectively. Model 5 and 6 predict thermal expansion along X and Y directions, respectively.

	Case 1		Case 2		Case 3	
	Model 1	Model 2	Model 3	Model 4	Model 5	Model 6
Test Loss	0.0003	0.0002	0.0007	0.0007	0.0005	0.0003
R square value	0.9711	0.9591	0.9270	0.9124	0.8653	0.9373

Table 1
Details of model training for the two benchmark cases.

Case	Basic Model	Label	Optimizer	Batch Size	Epochs	Learning ratio
1	ResNet−18	Normalized	Adam	32	100	Decreased by epochs
2	ResNet−18	Normalized	Adam	32	50	Decreased by epochs
3	ResNet−18	Normalized	Adam	32	50	Decreased by epochs

Table 3
Properties of each material phase and model parameters used in the two benchmark cases.

	Case 1 & Case 2			Case 3			
	Modulus (MPa)	Poisson's ratio	Density	Modulus (MPa)	Poisson ratio	Density	Coefficient of Thermal Expansion
MAT 1	379300	0.3	1.0	68300	0.33	1.0	23.6e−6
MAT 2	68300	0.3	1.0	0.1	0.25	1.0	1e−15

2.4. Implementation of the Grad-RAM

The Grad-RAM (Gradient-weighted Regression Activation Mapping) is an XAI approach that extends the Grad-CAM (Gradient-weighted Class Activation Mapping) approach to regression tasks. Originally devised for classification questions with discrete class labels, Grad-CAM operates by analyzing gradients flowing into the final convolutional layer relative to the score of the target class. However, in this study, where the prediction target is a continuous variable representing a microstructure property, gradients are computed with respect to the continuous output. Consequently, focus shifts towards understanding how variations in input image features influence the continuous output value. The process of conducting Grad-RAM on a CNN model is as follows.

1) Feed the input through the already-trained CNN to obtain the predicted regression value.

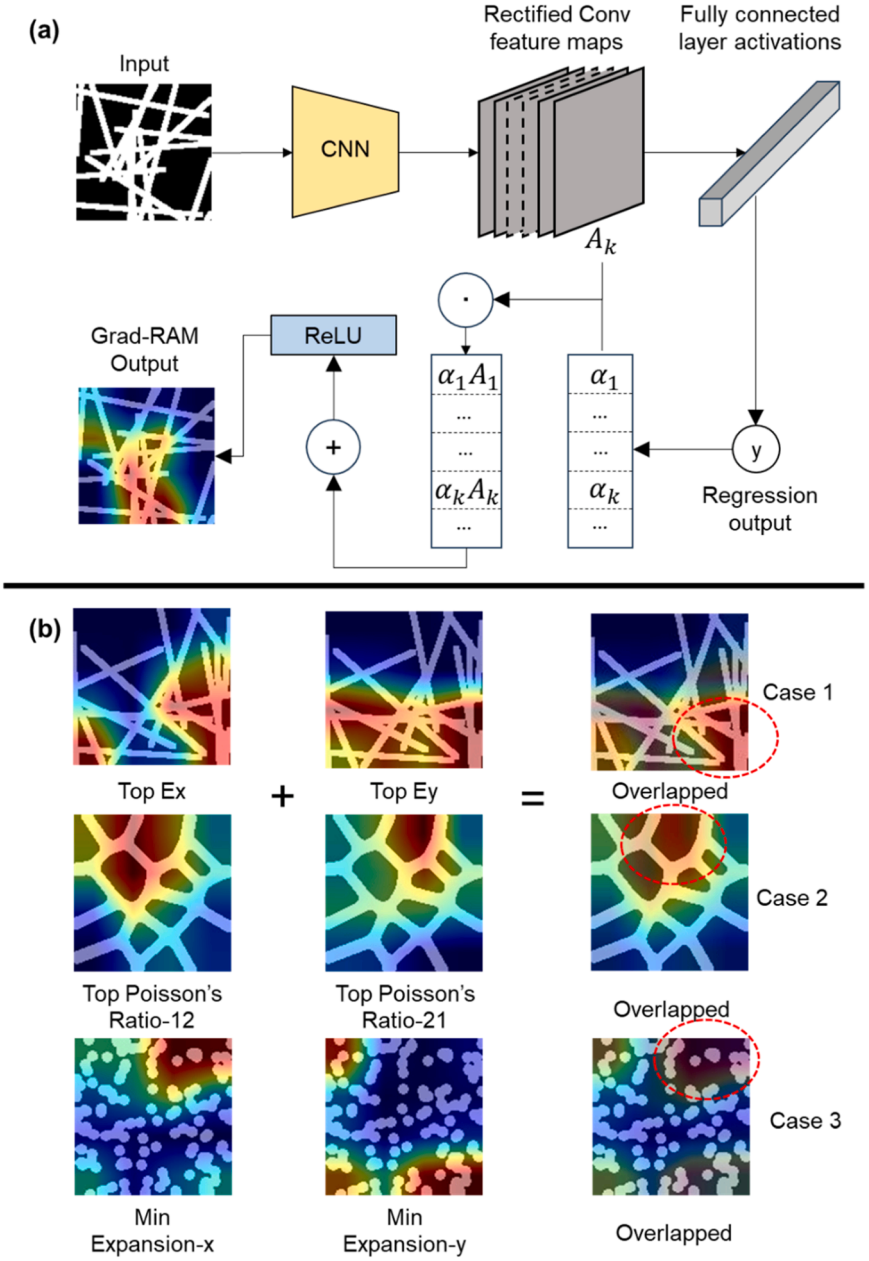

Fig. 3. (a) Architecture of Grad-RAM; (b) Two examples of applying Grad-RAM to generate heatmaps that highlight the critical regions in the microstructure images.

2) Choose a convolutional layer for analysis. The reason for selecting the last layer is that the layers deeper in the network capture more abstract features globally pertinent to the regression task.
3) With the selected layer, compute gradients of the regression value with respect to the feature maps of the selected convolutional layer.
4) Perform global average pooling on these gradients to obtain the importance weights of each feature map channel.
5) Create a weighted sum of the feature maps based on these importance weights, yielding a coarse heatmap matching the dimensions of the original image.
6) Apply ReLU activation to this heatmap. Positive values on this heatmap denote areas significantly influencing the increase in the output value.

Fig. 3a illustrates the flowchart of this process, and Fig. 3b presents two examples of Grad-RAM outputs on stochastic microstructure images. These outputs are heatmaps that highlight the critical regions. In the three presented benchmark cases, the outputs are the mechanical properties along the X and Y directions, respectively. Therefore, we employ Grad-RAM to generate a heatmap for each output and then intersect the two heatmaps to identify the final critical region.

2.5. Construction of new microstructure designs with key features identified by XAI

The heatmaps, originally grayscale images, are visualized as RGB images in Fig. 3 for easier interpretation. By binarizing the heatmap, we can identify a local patch containing the critical microstructure features from the original microstructure image. However, the local patch may not possess the target volume fraction. To facilitate volume fraction adjustment while preserving the topological characteristics of critical microstructure features, we propose to represent the material phase with a higher stiffness and Poisson's ratio (for benchmark Case 1 and 2) or a larger thermal expansion coefficient (for benchmark Case 3) in the bi-phase microstructure using its skeleton. The critical local microstructure feature in skeleton format, which serves as the microstructure unit for construction new designs, is obtained by masking the skeletonized microstructure image with the binarized heatmap. In order to ensure the connectivity of materials at the unit boundaries, we propose and compare two methods for constructing new metamaterial designs with microstructure units and select the mirroring method for its better performance (Figure S6).

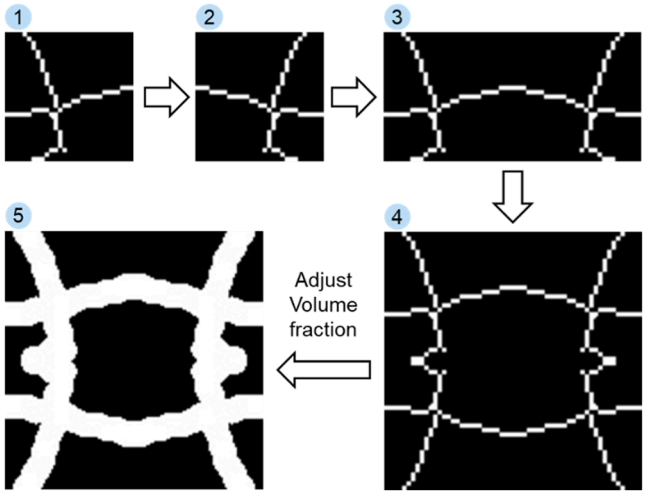

Fig. 4. Constructing novel microstructure designs utilizing key microstructure features identified by XAI: mirroring method.

- Mirroring method. The microstructure unit is treated as a quarter of the new design, which can be obtained by mirroring, following the process shown in Fig. 4.
- Graph-Based method. The skeleton in the microstructure unit is converted into a node-edge graph, as shown in Figure S5. The positions of the boundary nodes are adjusted (moved along the boundary) to ensure connections with a periodic boundary condition. This method is presented in the Supplementary Information.

After constructing the connected skeleton structure, the last step is to adjust the volume fraction of the binary image by adding white pixels to the skeleton. Details of the volume fraction adjustment process is provided in the Supplementary Information (Figure S7).

3. Results validation and discussion

3.1. Benchmark cases of microstructure design and generation of novel periodic microstructure designs

The effectiveness of proposed XAI-based framework is demonstrated on three benchmark cases: (1) design for high stiffness, (2) design for high Poisson's ratio, and (3) design for negative thermal expansion. The samples in the microstructure database are considered as bi-phase composites.

The design objective of Case 1 is to maximize Young's modulus along both the X and Y directions, under the constraint that the difference between them is less than 10 % of the smaller modulus value. The design objective of Case 2 is to maximize the Poisson's ratio along both X and Y directions, under the constraint that the difference between them is less than 10 % of the smaller value. There are two material phases in each microstructure sample, where the white phase represents Boron, and the black phase is Aluminum. The volume fraction of the white phase in the obtained designs should be within the range of 0.39–0.40. Young's moduli of the microstructure are obtained through the analysis of strain energy from simulated compression tests. For Case 3, design for minimum thermal expansion ratio, the design objective is minimizing the thermal expansion in X and Y directions, while the difference between them should be less than 10 % of the relatively smaller one. There are two material phases in each microstructure sample, where the white phase represents Aluminum, and the black phase is a certain type of foam, which has a lower stiffness and lower thermal expansion ratio. The volume fraction of the white phase in the obtained designs should be between 0.39 and 0.40. A temperature field is applied to the microstructure model, simulating the process of raising temperature from 20 to 500 °C to observe the behavior of thermal expansion along X and Y directions. The boundary conditions of the three benchmark cases are illustrated in Fig. 5a and 5b.

The mechanical properties of interest, including stiffness, Poisson's ratio, and thermal expansion, are obtained by simulations for all stochastic microstructure samples in the database. In Case 1, stochastic microstructure samples with exceptional stiffness, characterized by the top 10 % E_x and E_y values, are selected as exceptional outliers. In Case 2, stochastic microstructure samples with top 10 % Poisson's ratio are selected as the exceptional outliers. In Case 3, stochastic microstructure samples with bottom 10 % thermal expansion displacements are selected as the exceptional outliers. With the exceptional outliers, the proposed design framework is employed to generate novel periodic microstructure designs with favorable properties. Fig. 5c-e depict the four steps of design generation, showcasing the original images, skeletonized microstructure features within the critical region, the novel microstructure design in skeleton format, and finally, the complete microstructure design with the target volume fraction.

3.2. Validation of the XAI-generated novel microstructure designs

By comparing the XAI-generated periodic microstructure designs

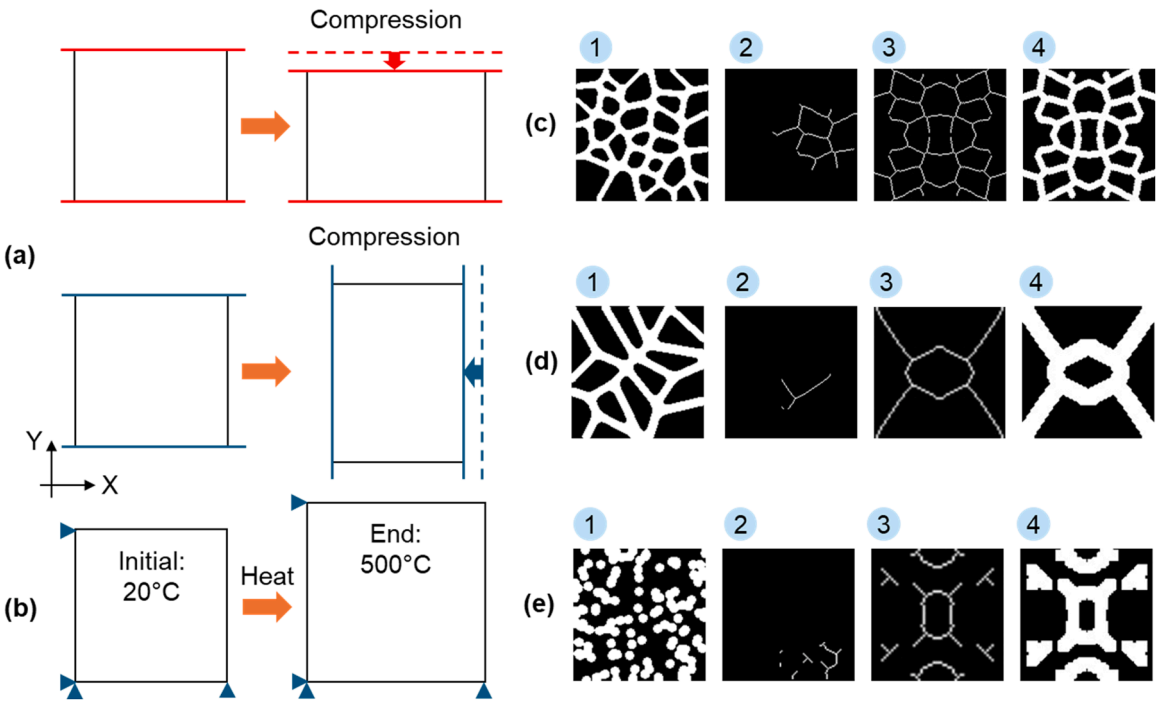

Fig. 5. Benchmark design cases and examples of novel microstructure designs generated by the proposed framework. (a) Boundary conditions used in both Case 1 and 2. (b) Boundary conditions used in Case 3. (c) Design generation process for Case 1: maximizing the Young's modulus along X and Y directions. (d) Design generation process for Case 2: maximizing the Poisson's ratio along X and Y directions. (e) Design generation process for Case 3: minimizing thermal expansion along X and Y directions.

with all stochastic microstructures in the training database, we confirm that this framework has the capability of generating design with unprecedented properties. In Fig. 6, the blue and yellow dots represent stochastic microstructure samples in the database, and the yellow dots are the exceptional outliers that are used in the XAI-based critical local feature identification. The red dots represent the periodic cellular metamaterial designs created based on the critical local features, which are also meeting the design constraints discussed in the previous section. The dashed lines in the plots represent points with the equal stiffness/thermal expansion. In the plots, the properties of the XAI-generated designs are obtained using the same simulation model employed for the stochastic microstructure samples. It is evident that the XAI-generated periodic microstructures achieve unprecedented properties, surpassing all known stochastic samples in the database, in all three test cases.

Further design validations are provided in the Supplementary Information (Figure S1 and S2). We provide comparisons between the XAI-generated metamaterial designs and those obtained by gradient-based topology optimization (TO), a well-established method for design for stiffness [72,73] and Poisson's ratio [74,75]. We find that the proposed framework can find designs that closely resemble the optimal designs by TO. Furthermore, by using XAI-generated designs as starting points, gradient-based TO achieves the local optimum faster compared to those starting from random images, which indicate a potential synergy between the XAI-based design framework and the gradient-based TO methodology. For the case of designing for minimal thermal expansion, we compare the XAI-generated designs with bi-phase metamaterial designs reported in the literature and confirm the superior performance of the XAI-generated designs.

3.3. Further notes on (i) adaptability of the framework and (ii) design generation with moderate samples

In Section 5 of the Supplementary Information, we demonstrated the adaptability of the proposed framework on an additional case study with different constituent material properties and a smaller dataset. In Section 6 of the Supplementary Information, we also present an investigation of the impact of heatmap binarization threshold on the performances of the obtained microstructure designs. By increasing the binarization threshold, the size of the identified critical region shrinks, meaning the identified microstructural features become more localized. In the presented case studies, more localized microstructural features lead to better performances generally, while we caution that an overly small critical region may result in microstructural features that are too small to be meaningful.

In Section 7 of the Supplementary Information, we applied the proposed framework to generate new designs using stochastic samples with moderate properties, excluding the exceptional outliers from the stochastic dataset. The purpose is to determine whether XAI can still identify critical features for generating high-performance designs. Our results in Figure S11 show that designs generated from moderate samples exhibit lower properties compared to those generated from exceptional outliers, though one of the designs from the moderate samples surpasses all stochastic samples. The results suggest that while it is less likely, it is still possible to identify advantageous microstructural features from moderate samples.

4. Conclusion

This paper introduced a new XAI-based design framework that identifies advantageous features from stochastic microstructure samples and generates novel periodic microstructures with enhanced properties. The effectiveness of this framework is demonstrated through the successful generation of novel designs exhibiting superior properties compared to all known samples within the existing dataset. This work highlights the transformative potential of XAI in surpassing the limitations of traditional ad hoc design processes, which typically rely on human expertise and brainstorming to transfer knowledge learned from one category of microstructures to inspire novel designs in another category (e.g., from stochastic to periodic). The proposed design

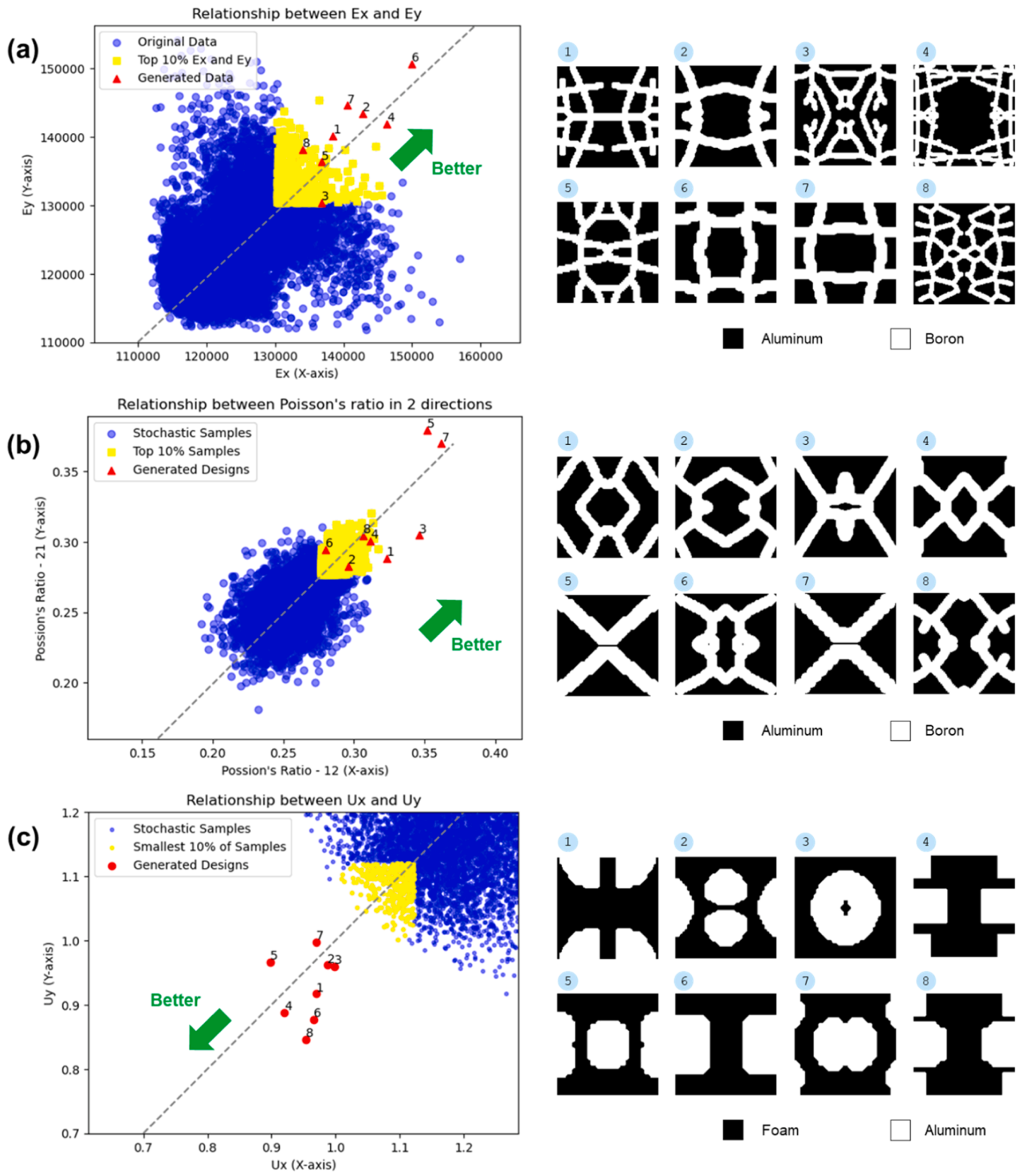

Fig. 6. Design validation: Comparison between the XAI-generated microstructure designs and all stochastic microstructure samples in the database. (a) Case 1: Design for maximum stiffness along X and Y directions. (b) Case 2: Design for maximum Poisson's ratio. (c) Case 3: Design for minimum thermal expansion.

framework enables design automation and reduces the reliance on human judgment and brainstorming. The results validate the hypothesis that by learning advantageous microstructure features from stochastic microstructures using XAI, novel periodic microstructure designs created by arranging those advantageous features in a periodic manner can achieve superior properties compared to stochastic microstructures.

The limitations of the proposed framework will be explored in our future work. The Grad-RAM approach primarily focuses on identifying local microstructure features, potentially overlooking high-level spatial distribution patterns of material phases. However, certain material properties might not be exclusively sensitive to local features. In our future research, we plan to improve the framework to enable the

identification of high-level patterns, such as spatial distribution patterns, that positively influence the properties of interest for the generative design of novel structures. In addition to designing metamaterials, we plan to extend this method to porous microstructures, where complete connectivity of the solid phase is a crucial geometric constraint that was not addressed in this work. We also aim to apply this method to the design of flexible structures with large deformations to achieve desired dynamic behaviors.

CRediT authorship contribution statement

Zhengkun Feng: Writing – review & editing, Writing – original draft, Methodology, Investigation. **Leidong Xu:** Writing – review & editing, Writing – original draft, Methodology, Investigation. **Weijun Lei:** Writing – review & editing, Writing – original draft, Methodology, Investigation. **Hongyi Xu:** Writing – review & editing, Writing – original draft, Supervision, Funding acquisition, Conceptualization. **Shikui Chen:** Writing – review & editing, Writing – original draft, Supervision, Funding acquisition.

Declaration of Competing Interest

The authors declare the following financial interests/personal relationships which may be considered as potential competing interests: Hongyi Xu reports financial support was provided by National Science Foundation. If there are other authors, they declare that they have no known competing financial interests or personal relationships that could have appeared to influence the work reported in this paper.

Acknowledgements

ZF and HX gratefully acknowledge financial support from the National Science Foundation (CAREER Award CMMI-2142290). WL and SC gratefully acknowledge financial support from the National Science Foundation (PFI-RP-2213852).

Appendix A. Supporting information

Supplementary data associated with this article can be found in the online version at doi:10.1016/j.eml.2024.102269.

Data availability

Data will be made available on request.

References

[1] H. Xu, et al., Descriptor-based methodology for statistical characterization and 3D reconstruction of microstructural materials, Comput. Mater. Sci. 85 (2014) 206–216.
[2] C.M. Breneman, et al., Stalking the materials genome: a data-driven approach to the virtual design of nanostructured polymers, Adv. Funct. Mater. 23 (46) (2013) 5746–5752.
[3] H. Xu, et al., A descriptor-based design methodology for developing heterogeneous microstructural materials system, J. Mech. Des. 136 (5) (2014) 051007.
[4] Z. Chen, et al., Multiscale finite element modeling of sheet molding compound (SMC) composite structure based on stochastic mesostructure reconstruction, Compos. Struct. 188 (2018) 25–38.
[5] Z. Chen, et al., Failure of chopped carbon fiber Sheet Molding Compound (SMC) composites under uniaxial tensile loading: computational prediction and experimental analysis, Compos. Part A: Appl. Sci. Manuf. 118 (2019) 117–130.
[6] H. Xu, et al., Microstructure reconstruction of battery polymer separators by fusing 2D and 3D image data for transport property analysis, J. Power Sources 480 (2020) 229101.
[7] H. Xu, C. Bae, Stochastic 3D microstructure reconstruction and mechanical modeling of anisotropic battery separators, J. Power Sources 430 (2019) 67–73.
[8] H. Xu, et al., Mechanical modeling of battery separator based on microstructure image analysis and stochastic characterization, J. Power Sources 345 (2017) 137–145.
[9] Z. Pan, et al., Microstructural deformation patterns of a highly orthotropic polypropylene separator of lithium-ion batteries: mechanism, model, and theory, Extrem. Mech. Lett. (2020) 100705.
[10] M. Saha, et al., Effect of density, microstructure, and strain rate on compression behavior of polymeric foams, Mater. Sci. Eng.: A 406 (1-2) (2005) 328–336.
[11] C. Huang, P.S. Grant, Coral-like directional porosity lithium ion battery cathodes by ice templating, J. Mater. Chem. A 6 (30) (2018) 14689–14699.
[12] J.U. Surjadi, et al., Mechanical metamaterials and their engineering applications, Adv. Eng. Mater. 21 (3) (2019) 1800864.
[13] Z. Wang, et al., Design of phononic bandgap metamaterials based on Gaussian mixture beta variational autoencoder and iterative model updating, J. Mech. Des. 144 (4) (2022) 041705.
[14] D.W. Rosen, S.R. Johnston, M. Reed, Design of general lattice structures for lightweight and compliance applications (2006).
[15] M. Montemurro, G. Bertolino, T. Roiné, A general multi-scale topology optimisation method for lightweight lattice structures obtained through additive manufacturing technology, Compos. Struct. 258 (2021) 113360.
[16] M.C. Fernandes, et al., Mechanically robust lattices inspired by deep-sea glass sponges, Nat. Mater. 20 (2) (2021) 237–241.
[17] N. San Ha, G. Lu, A review of recent research on bio-inspired structures and materials for energy absorption applications, Compos. Part B: Eng. 181 (2020) 107496.
[18] L. Grunenfelder, et al., Bio-inspired impact-resistant composites, Acta Biomater. 10 (9) (2014) 3997–4008.
[19] N.K. Katiyar, et al., Nature-inspired materials: emerging trends and prospects, NPG Asia Mater. 13 (1) (2021) 56.
[20] D. Lehmhus, et al., From stochastic foam to designed structure: balancing cost and performance of cellular metals, Materials 10 (8) (2017) 922.
[21] D. Nepal, et al., Hierarchically structured bioinspired nanocomposites, Nat. Mater. 22 (1) (2023) 18–35.
[22] M.P. Bendsøe, N. Kikuchi, Generating optimal topologies in structural design using a homogenization method, Comput. Methods Appl. Mech. Eng. 71 (2) (1988) 197–224.
[23] O. Sigmund, On the design of compliant mechanisms using topology optimization, J. Struct. Mech. 25 (4) (1997) 493–524.
[24] W. Zuo, K. Saitou, Multi-material topology optimization using ordered SIMP interpolation, Struct. Multidiscip. Optim. 55 (2) (2017) 477–491.
[25] M.Y. Wang, X. Wang, D. Guo, A level set method for structural topology optimization, Comput. Methods Appl. Mech. Eng. 192 (1-2) (2003) 227–246.
[26] Y. Wang, et al., Level-set topology optimization for multimaterial and multifunctional mechanical metamaterials, Eng. Optim. 49 (1) (2017) 22–42.
[27] M. Ebner, et al., X-ray tomography of porous, transition metal oxide based lithium ion battery electrodes, Adv. Energy Mater. 3 (7) (2013) 845–850.
[28] M. Kespe, H. Nirschl, Numerical simulation of lithium-ion battery performance considering electrode microstructure, Int. J. Energy Res. 39 (15) (2015) 2062–2074.
[29] A.N. Mistry, K. Smith, P.P. Mukherjee, Secondary-phase stochastics in lithium-ion battery electrodes, ACS Appl. Mater. Interfaces 10 (7) (2018) 6317–6326.
[30] Y. Jiao, F. Stillinger, S. Torquato, Modeling heterogeneous materials via two-point correlation functions: basic principles, Phys. Rev. E 76 (3) (2007) 031110.
[31] Y. Jiao, F.H. Stillinger, S. Torquato, Modeling heterogeneous materials via two-point correlation functions. II. Algorithmic details and applications, Phys. Rev. E 77 (3) (2008).
[32] S. Torquato, Optimal design of heterogeneous materials, Annu. Rev. Mater. Res. 40 (2010) 101–129.
[33] Y. Zhang, et al., High-throughput 3D reconstruction of stochastic heterogeneous microstructures in energy storage materials, npj Comput. Mater. 5 (1) (2019) 1–8.
[34] S. Yu, et al., Design of non-deterministic quasi-random nanophotonic structures using Fourier space representations, Sci. Rep. 7 (1) (2017) 1–10.
[35] A. Iyer, et al., Designing anisotropic microstructures with spectral density function, Comput. Mater. Sci. 179 (2020) 109559.
[36] J.A. Quiblier, A new 3-dimensional modeling technique for studying porous-media, J. Colloid Interface Sci. 98 (1) (1984) 84–102.
[37] M. Grigoriu, Random field models for two-phase microstructures, J. Appl. Phys. 94 (6) (2003) 3762–3770.
[38] C.T. Chen, G.X. Gu, Generative deep neural networks for inverse materials design using backpropagation and active learning, Adv. Sci. (Weinh.) 7 (5) (2020) 1902607.
[39] L. Wang, et al., Deep generative modeling for mechanistic-based learning and design of metamaterial systems, Comput. Methods Appl. Mech. Eng. 372 (2020) 113377.
[40] Y. Mao, Q. He, X. Zhao, Designing complex architectured materials with generative adversarial networks, Sci. Adv. 6 (17) (2020) eaaz4169.
[41] X. Li, et al., Designing phononic crystal with anticipated band gap through a deep learning based data-driven method, Comput. Methods Appl. Mech. Eng. 361 (2020) 112737.
[42] H. Zhang, et al., Accelerated topological design of metaporous materials of broadband sound absorption performance by generative adversarial networks, Mater. Des. 207 (2021) 109855.
[43] H.T. Kollmann, et al., Deep learning for topology optimization of 2D metamaterials, Mater. Des. 196 (2020) 109098.
[44] J. Jung, et al., Microstructure design using machine learning generated low dimensional and continuous design space, Materialia (2020) 100690.
[45] R. Cang, et al., Improving direct physical properties prediction of heterogeneous materials from imaging data via convolutional neural network and a morphology-aware generative model, Comput. Mater. Sci. 150 (2018) 212–221.
[46] S. Sundar, V. Sundararaghavan, Database development and exploration of process–microstructure relationships using variational autoencoders, Mater. Today Commun. (2020) 101201.

[47] Z. Yang, et al., Microstructural materials design via deep adversarial learning methodology, J. Mech. Des. 140 (11) (2018).
[48] R.K. Tan, N.L. Zhang, W. Ye, A deep learning–based method for the design of microstructural materials. Struct. Multidiscip. Optim. (2019) 1–22.
[49] X. Zheng, et al., Controllable inverse design of auxetic metamaterials using deep learning, Mater. Des. 211 (2021) 110178.
[50] A. Samaei, S. Chaudhuri, Mechanical performance of zirconia-silica bilayer coating on aluminum alloys with varying porosities: deep learning and microstructure-based FEM, Mater. Des. 207 (2021) 109860.
[51] L. Xu, et al., Harnessing structural stochasticity in the computational discovery and design of microstructures, Mater. Des. 223 (2022) 111223.
[52] L. XU, K.Naghavi Khanghah, H. Xu, Design of Mixed-Category Stochastic Microstructures: A Comparison of Curvature Functional-based and Deep Generative Model-based Methods. ASME 2023 International Design Engineering Technical Conferences & Computers and Information in Engineering Conference, American Society of Mechanical Engineers, Boston, 2023.
[53] L. Xu, K. Naghavi Khanghah, H. Xu, Designing mixed-category stochastic microstructures by deep generative model-based and curvature functional-based methods, J. Mech. Des. 146 (4) (2024).
[54] L.H. Gilpin, et al., Explaining explanations: An overview of interpretability of machine learning. 2018 IEEE 5th International Conference on data science and advanced analytics (DSAA), IEEE, 2018.
[55] A.B. Arrieta, et al., Explainable Artificial Intelligence (XAI): Concepts, taxonomies, opportunities and challenges toward responsible AI, Inf. Fusion 58 (2020) 82–115.
[56] Wang, Z. and J. Yang, *Diabetic retinopathy detection via deep convolutional networks for discriminative localization and visual explanation*. arXiv preprint arXiv: 1703.10757, 2017.
[57] G. Qu, et al., Ensemble manifold regularized multi-modal graph convolutional network for cognitive ability prediction, IEEE Trans. Biomed. Eng. 68 (12) (2021) 3564–3573.
[58] Y. Li, et al., Stochastic reconstruction and microstructure modeling of SMC chopped fiber composites, Compos. Struct. 200 (2018) 153–164.
[59] H. Xu, et al., Guiding the design of heterogeneous electrode microstructures for Li-ion batteries: microscopic imaging, predictive modeling, and machine learning, Adv. Energy Mater. 11 (19) (2021) 2003908.
[60] H. Xu, et al., Data-Driven Multiscale Science for Tire Compounding: Methods and Future Directions. Theory and Modeling of Polymer Nanocomposites, Springer, 2021, pp. 281–312.
[61] K. He, et al., Deep residual learning for image recognition, Proceedings of the IEEE conference on computer vision and pattern recognition (2016).
[62] M. Yang, et al., New algorithms for virtual reconstruction of heterogeneous microstructures, Comput. Methods Appl. Mech. Eng. 338 (2018) 275–298.
[63] S. Hein, et al., Stochastic microstructure modeling and electrochemical simulation of lithium-ion cell anodes in 3D, J. Power Sources 336 (2016) 161–171.
[64] S. Falco, et al., Generation of 3D polycrystalline microstructures with a conditioned Laguerre-Voronoi tessellation technique, Comput. Mater. Sci. 136 (2017) 20–28.
[65] S. Yu, et al., Characterization and design of functional quasi-random nanostructured materials using spectral density function, J. Mech. Des. 139 (7) (2017) 071401.
[66] C. Yeong, S. Torquato, Reconstructing random media, Phys. Rev. E 57 (1) (1998) 495.
[67] C. Yeong, S. Torquato, Reconstructing random media. II. Three-dimensional media from two-dimensional cuts, Phys. Rev. E 58 (1) (1998) 224.
[68] S. Torquato, G. Stell, Microstructure of two-phase random media. I. The n-point probability functions. J. Chem. Phys. 77 (4) (1982) 2071–2077.
[69] Y. Liu, et al., Computational microstructure characterization and reconstruction for stochastic multiscale material design, Comput. -Aided Des. 45 (1) (2013) 65–76.
[70] C. Chatfield, H. Xing, The analysis of time series: an introduction with R, CRC Press, 2019.
[71] N. Berk, Scattering properties of a model bicontinuous structure with a well defined length scale, Phys. Rev. Lett. 58 (25) (1987) 2718.
[72] A. Takezawa, Y. Koizumi, M. Kobashi, High-stiffness and strength porous maraging steel via topology optimization and selective laser melting, Addit. Manuf. 18 (2017) 194–202.
[73] L. Zhang, et al., Topology-optimized lattice structures with simultaneously high stiffness and light weight fabricated by selective laser melting: design, manufacturing and characterization, J. Manuf. Process. 56 (2020) 1166–1177.
[74] P. Vogiatzis, et al., Topology optimization of multi-material negative Poisson's ratio metamaterials using a reconciled level set method, Comput. -Aided Des. 83 (2017) 15–32.
[75] A. Clausen, et al., Topology optimized architectures with programmable Poisson's ratio over large deformations, Adv. Mater. 27 (37) (2015) 5523–5527.